2. Diagnostic Techniques

Several diagnostic techniques have been examined that can provide information about material distribution in multiphase flows. These diagnostic techniques differ both in the physical effect employed to infer material distribution and in the degree of spatial and temporal resolution that can be achieved. Two broad classes of diagnostics can be defined depending on the degree of spatial resolution that is achieved: (1) those diagnostics yielding only spatially-averaged or local information; and (2) those diagnostics yielding spatially resolved information. The first class of diagnostics includes level-rise (LR) measurements, differential-pressure (DP) measurements, bulk electrical impedance (BEI) measurements, electrical bubble probes (EBPs), optical bubble probes, heat-injection probes, and acoustical bubble probes. Of these seven techniques, the first four are examined herein. The second class of diagnostics includes x-ray tomography (XRT), gamma-densitometry tomography (GDT), electrical-impedance tomography (EIT), and acoustical tomography. Of these four diagnostics, the first is used for validation purposes, the second and third are examined extensively, and the fourth has not been investigated.

2.1. Techniques Yielding Spatially-Averaged or Local Information

Diagnostic techniques yielding spatially-averaged or local material-distribution information for multiphase flows are useful while attempting to develop and validate more advanced noninvasive diagnostics capable of providing spatially resolved material distribution. Four such techniques have been employed in this capacity: level-rise (LR) measurements, differential-pressure (DP) measurements, bulk electrical impedance (BEI) measurements, and electrical bubble probes (EBPs). The first three provide volume-averaged values of material volume fractions over a significant region of the flow, whereas the last technique provides a local measurement of material volume fractions.

2.1.1. Level-Rise (LR) Technique

The level-rise (LR) technique is discussed here in the context of a gas-liquid bubble-column flow, as shown in Figure 6. It is a conceptually simple technique that relies on the incompressibility of the liquid portion of the multiphase flow and provides a value for the gas and liquid volume fractions averaged over the entire volume of the bubble column. The height H_0 of the gas-liquid interface above the bottom of the column is measured in the absence of gas flow, and the expanded height H is measured in the presence of gas flow. When the bubble column has a constant cross-sectional area, the volume-averaged values of the gas and liquid volume fractions are given by the relations

$$\varepsilon_G = 1 - \frac{H_0}{H} \text{ and } \varepsilon_L = \frac{H_0}{H}. \quad (3)$$

The expanded height can be measured either visually or by using a video camera and image-processing software. The principal source of uncertainty for this technique is that the gas-liquid interface during gas flow is neither flat nor stationary in time. The combination of these two features precludes the use of common image-processing techniques to reduce this uncertainty. Thus, in this study, visual observation is used to estimate the expanded height during gas flow. Extension of this technique to more than two phases is straightforward, but additional information is then required to determine the volume fractions of all phases unambiguously.

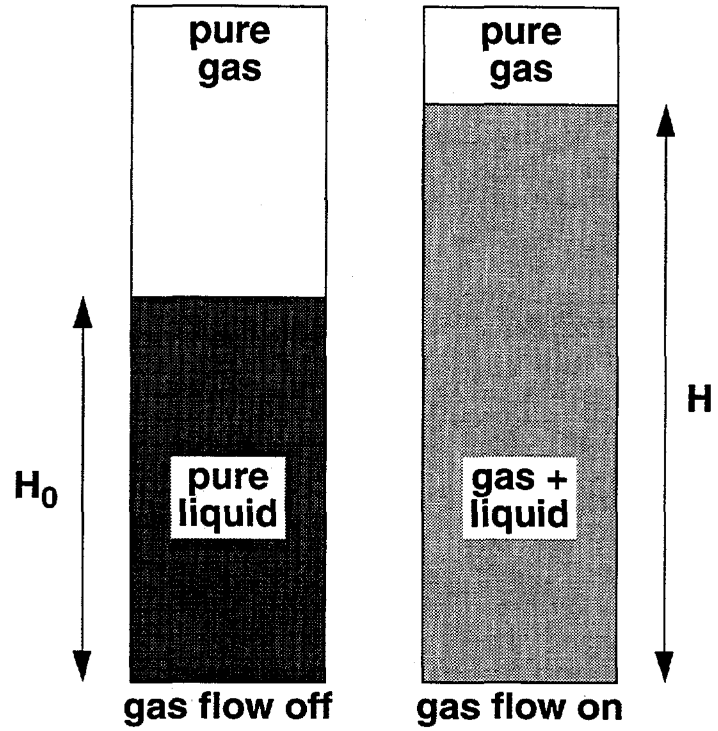

Figure 6. Schematic diagram of level-rise (LR) technique.

2.1.2. Differential-Pressure (DP) Technique

The differential-pressure (DP) technique is discussed here in the context of a gas-liquid bubble-column flow, as shown in Figure 7. This technique requires a gravitational field (as does the bubble-column flow itself) and yields a value for the gas and liquid volume fractions averaged over the region of the bubble column between two vertically offset pressure transducers. The pressure difference ΔP is measured between two pressure transducers separated by a distance W, and the measured pressure gradient is assumed to be purely hydrostatic at the average density of the gas-liquid mixture:

$$\Delta P = (\varepsilon_G \rho_G + \varepsilon_L \rho_L) g W \text{ and } \varepsilon_G + \varepsilon_L = 1, \quad (4)$$

where ρ_G and ρ_L are the gas and liquid densities and g is the gravitational acceleration. These relations allow determination of the gas and liquid volume fractions:

$$\varepsilon_G = \frac{\rho_L g W - \Delta P}{(\rho_L - \rho_G) g W} \text{ and } \varepsilon_L = \frac{\Delta P - \rho_G g W}{(\rho_L - \rho_G) g W}. \quad (5)$$

Due to the presence of pressure fluctuations due to flow unsteadiness, these relations are applied only in the time-averaged sense. Also, the gas density is often neglected since it is typically 2-3 orders of magnitude smaller than the liquid density. The principal source of uncertainty for this technique lies in the basic assumption that the time-averaged pressure gradient is hydrostatic. This assumption constrains the time-averaged liquid-acceleration and wall-shear contributions to the pressure gradient to be small compared to the hydrostatic contribution. The former constraint requires that the time-averaged velocity and volume-fraction fields vary slowly in the vertical direction. This requirement would be satisfied if these fields approached their "fully developed" distributions, which is believed to occur within a few vessel diameters above the point of gas injection. However, this requirement may not be true near the bottom of the bubble column or near the gas-liquid interface, where the liquid is strongly accelerated and actually reverses its direction of flow. While difficult to quantify, the latter constraint suggests operation at high Reynolds numbers (small viscosity). However, it should be emphasized that wall shear does not vanish for turbulent flow in the limit of zero viscosity. Since the Reynolds numbers under consideration are on the order of 10^3-10^6, viscous wall shear appears acceptably small, but multiphase turbulent wall shear is difficult to assess. Extension of this technique to more than two phases is straightforward, but additional information is then required to determine the volume fractions of all phases unambiguously.

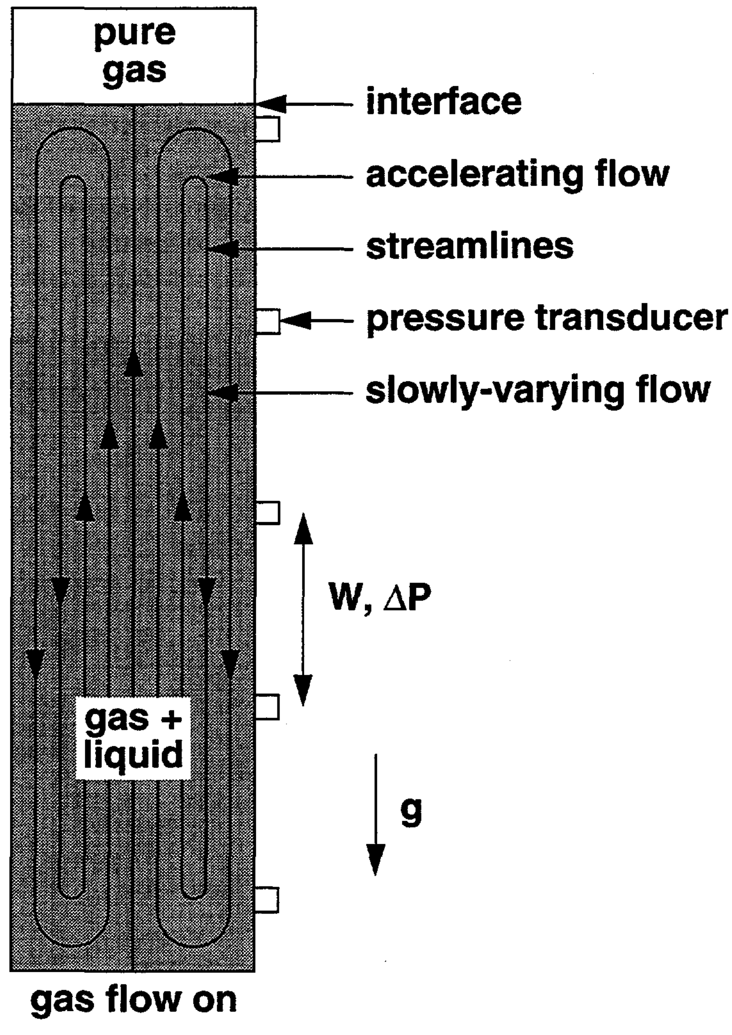

Figure 7. Schematic diagram of differential-pressure (DP) technique.

2.1.3. Bulk Electrical Impedance (BEI) Technique

The bulk electrical-impedance (BEI) technique is discussed here in the context of a gas-liquid bubble-column flow. This technique depends on the liquid having a much greater electrical conductivity than the gas and yields a value for the gas and liquid volume fractions averaged over an ill-defined region of the bubble column between two oppositely-positioned large-area electrodes. The gas-liquid mixture is assumed to be a resistive medium with a mixture conductivity σ_m given by the Maxwell-Hewitt relation for a random dispersion of small insulating spheres (gas bubbles) within a continuum (the liquid) of conductivity σ_L (cf. Hewitt, 1978; Ceccio and George, 1996):

$$\frac{\sigma_m}{\sigma_L} = \frac{1-\varepsilon_G}{1+(\varepsilon_G/2)}. \tag{6}$$

This relation can be inverted to determine the gas and liquid volume fractions:

$$\varepsilon_G = \frac{1-(\sigma_m/\sigma_L)}{1+(1/2)(\sigma_m/\sigma_L)} \text{ with } \varepsilon_G + \varepsilon_L = 1. \tag{7}$$

These relations should be applied to instantaneous quantities but are typically applied using time-averaged quantities.

Figure 8 shows a typical BEI probe ring, which has two rectangular electrodes (3.8 cm tall, 120° in angular extent) positioned at opposite sides of the ring.

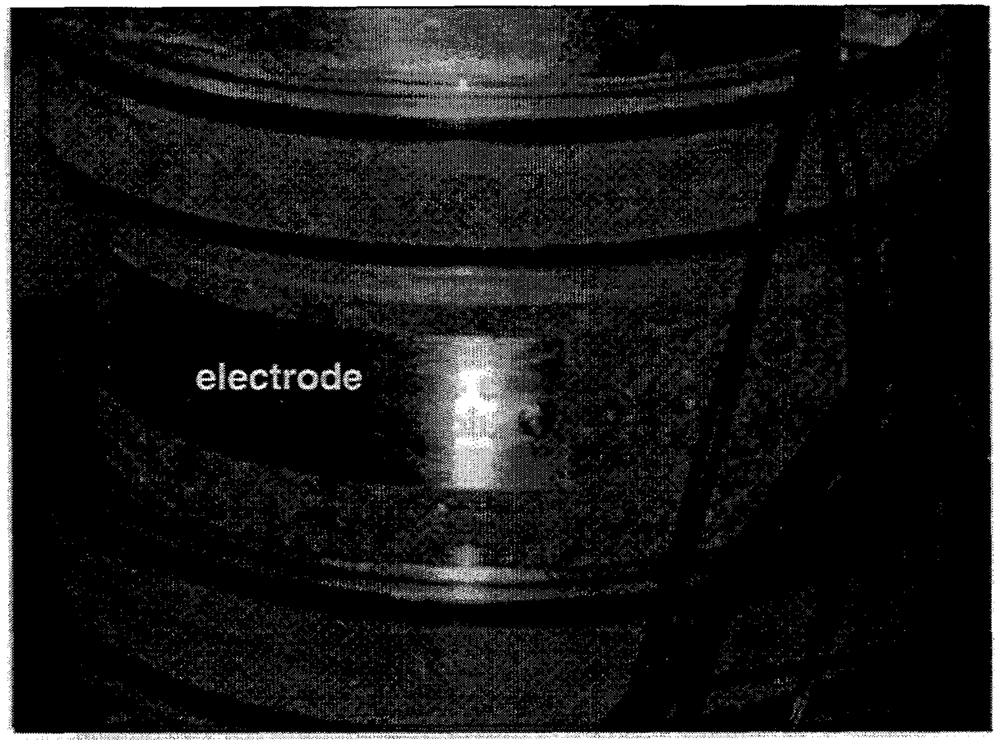

Figure 8. Bulk electrical impedance (BEI) probe ring with two rectangular electrodes.

In typical operation, neither the mixture conductivity nor the liquid conductivity is measured directly since this would require detailed knowledge of the voltage distribution within the mixture, which is particularly sensitive to various aspects of the electrode geometry such as corners and edges. Instead, a known alternating current (typically at frequencies around 50 kHz) is passed from one electrode to the other in the absence of gas flow and in the presence of gas flow, and the resulting voltage differences are measured for both cases. By virtue of Ohm's Law, the ratio of the mixture conductivity to the liquid conductivity is equal to the ratio of the voltage without gas flow to the voltage with gas flow. The principal sources of uncertainty for this technique lie in three areas: (1) the assumption of a spatially uniform distribution of gas volume fraction in measurement region; (2) the assumption of the Maxwell-Hewitt relation, which relies on spherical bubbles; and (3) the use of time-averaged quantities rather than instantaneous quantities. As will be shown in subsequent sections, a strong radial variation of gas volume fraction generally exists in bubble-column flows. It appears possible to "calibrate" the BEI technique by comparison with another technique for measuring gas volume fraction, but this calibration is not generic because it depends on the radial variation of the gas volume fraction present in the flow used for calibration. Moreover, for large gas volume fractions, bubble shapes may depart significantly from sphericity, so the Maxwell-Hewitt relation, which assumes spherical bubbles, becomes of questionable validity. Assessing the impact of time-averaging requires knowledge of the size of gas-volume-fraction fluctuations relative to the average gas volume fraction. This quantity is not believed to be large but cannot be measured at present. Because of the above considerations, it is best to use BEI with systems for which calibration is possible and for which conditions do not depart significantly from the conditions used for calibration. Extension of this technique to more than two phases is straightforward if all but one of the phases are both dispersed and insulating, but additional information is then required to determine the volume fractions of the dispersed insulating phases unambiguously.

2.1.4. Electrical Bubble Probe (EBP)

An electrical bubble probe (EBP) has been developed to make local measurements of gas volume fraction in gas-liquid bubble-column flow. A schematic diagram of an EBP is shown in Figure 9. This probe consists of two coaxial electrodes separated by insulating material mounted on a support. Since the bubbles travel predominately upward, the probe is oriented pointing downward. The voltage required to maintain a prescribed current between the electrodes is greatly increased when the probe intercepts a bubble, so the voltage history reveals the amounts of time the probe spends immersed in gas and in liquid. These times are interpreted as proportional to the gas and liquid volume fractions at the location of measurement. If the voltage observed with liquid immersion is much smaller than the voltage observed with gas immersion, then the rms of the voltage history is proportional to the gas volume fraction.

An EBP has been fabricated for which the outer electrode has a diameter of 1.27 mm (0.050 inch) and the distance from the inner electrode tip to the outer electrode edge is 0.635 mm (0.025 inch). This probe was inserted into the transparent bubble column (discussed later in this report), and voltage histories were recorded for several air flow rates. One voltage history is shown in Figure 9, and bubble interceptions are readily apparent. A comparison of the rms EBP voltage to the DP signal (where a value of 0 indicates a gas volume fraction of 0) is also shown in Figure 9. The good correlation indicates that EBPs can provide accurate gas-volume-fraction measurements. Radial gas volume fraction profiles, acquired by traversing the probe and assuming that the rms of the voltage history is proportional to the gas volume fraction, are shown in Figure 10. Cross sectional averages of these profiles are in good agreement with DP results (not shown). Although these results are encouraging, more effort is required to determine whether an EBP can be successfully applied to highly nondilute flow, to flows with wide ranges of bubble sizes, or to flows with more than two phases.

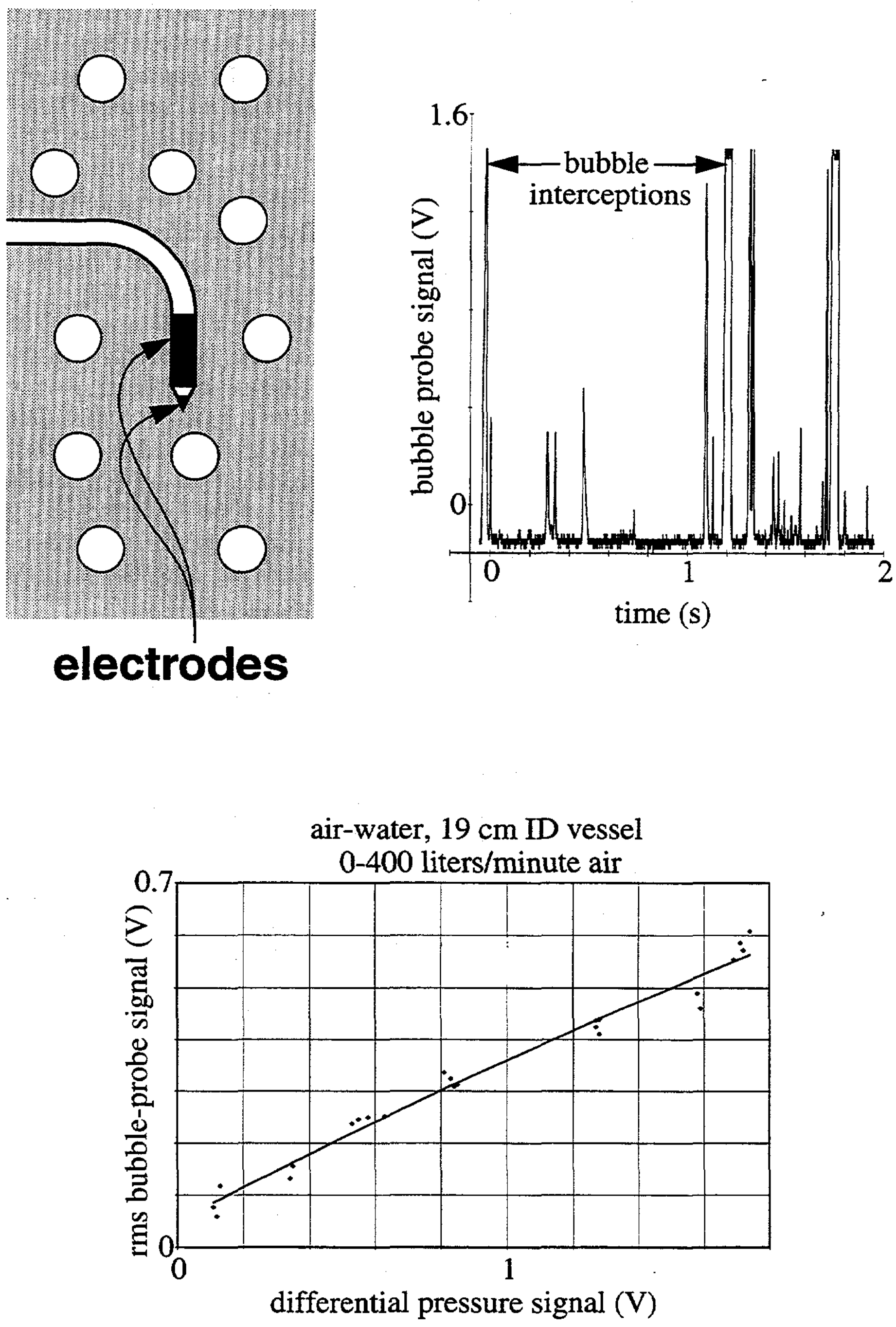

Figure 9. Electrical bubble probe (EBP) schematic, bubble interceptions, and rms correlation.

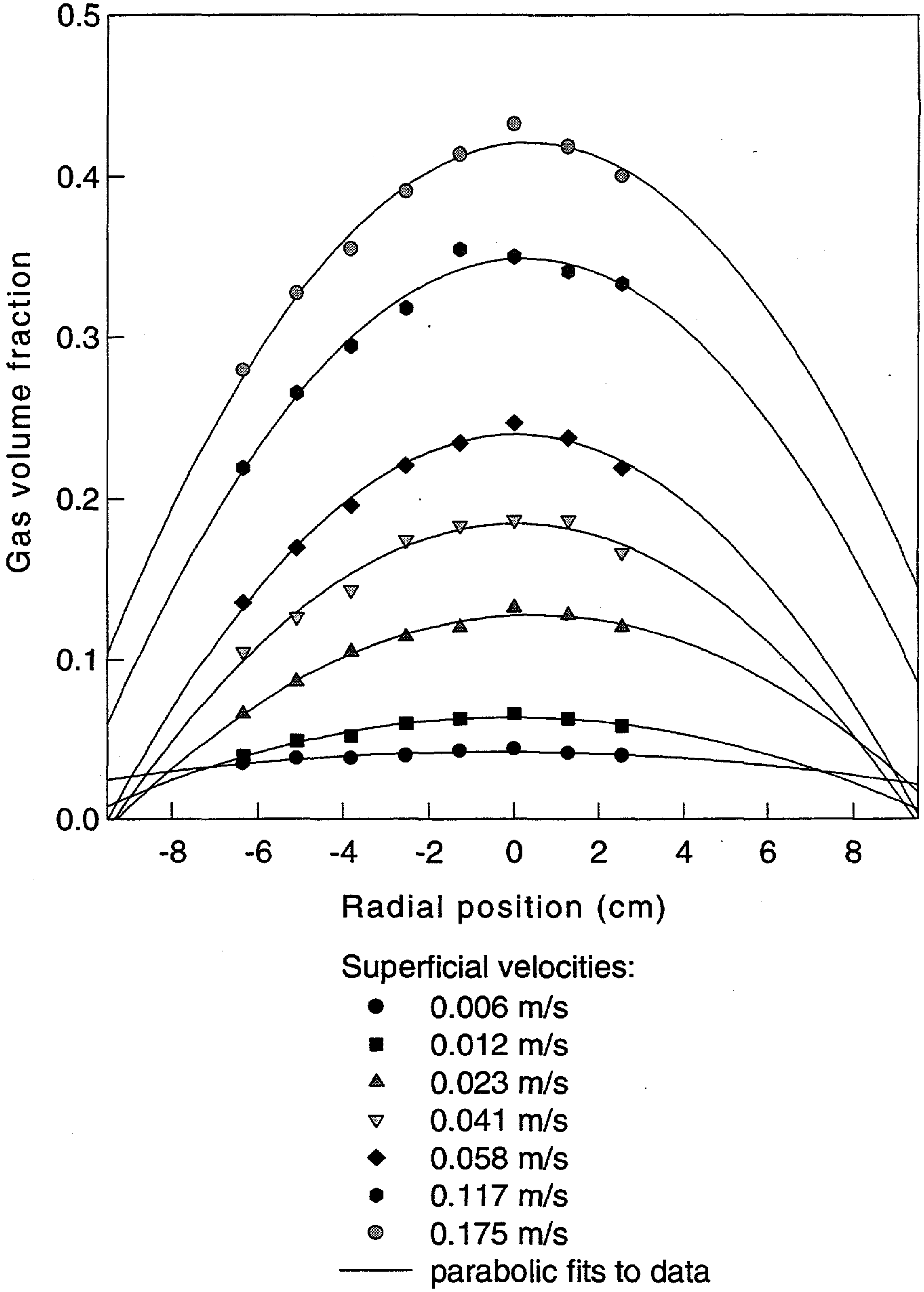

Figure 10. Gas volume fraction radial distributions from EBP.